Magnetic properties of layered complexes $[M(hfac)_2]_3(\mathbf{R})_2$, M = Mn(II) and Cu(II), with trisnitroxide radicals having various metal–radical exchange interactions

2001 J. Phys.: Condens. Matter 13 7429

(http://iopscience.iop.org/0953-8984/13/33/322)

INSTITUTE OF PHYSICS PUBLISHING JOURNAL OF PHYSICS: CONDENSED MATTER

J. Phys.: Condens. Matter **13** (2001) 7429–7442 PII: S0953-8984(01)23763-1

Magnetic properties of layered complexes $[M(hfac)_2]_3(R)_2$, M = Mn(II) and Cu(II), with trisnitroxide radicals having various metal–radical exchange interactions

Motoko Tanaka[1], **Yuko Hosokoshi**[1], **Ashot S Markosyan**[1,2,4], **Hizu Iwamura**[3] **and Katsuya Inoue**[1]

[1] Applied Molecular Science, Institute for Molecular Science, Nishigonaka 38, Myodaiji, Okazaki 444-8585, Japan
[2] Faculty of Physics, M V Lomonosov Moscow State University, 119899 Moscow, Russia
[3] Department of General Science, University of Air, 2-11, Wakaba, Mihama, Chiba, 261-8586, Japan

E-mail: marko@plms.phys.msu.su

Received 9 April 2001, in final form 19 June 2001
Published 2 August 2001
Online at stacks.iop.org/JPhysCM/13/7429

Abstract

A series of new layered 2D-network complexes $[M(hfac)_2]_3(\mathbf{R}_\Delta)_2$ of M = Mn(II) and Cu(II) with trisnitroxide radicals $\mathbf{R}_\Delta$ has been prepared and the magnetic properties were studied. Each triradical $\mathbf{R}_\Delta$ has a quartet ground state and contributes not only to the formation of extended structures but essentially to the overall magnetism. Several exchange interactions, between M and nitroxide and intraradical nitroxide–nitroxide interactions, are responsible for the development of the characteristic magnetic properties in these heterospin systems. Depending on the nature of the interlayer interactions, they show either ferro/ferrimagnetic or antiferromagnetic long range order. The hierarchy of the different exchange interactions is established and the Mn–nitroxide and Cu–nitroxide exchange integrals are evaluated from the analysis of the temperature dependence of the paramagnetic susceptibility. With increasing intraradical exchange interaction, the complexes exhibit more pronounced 2D behaviour.

1. Introduction

Among a large number of molecule based magnetic materials the heterospin systems consisting of 3d transition metal ions and organic free radicals as ligands are of special interest [1–4]. When the ligands employed have a non-zero spin ground state and more than one ligating site, extended structures such as one-dimensional (1D) chains and 2D and 3D networks can be

[4] Addressee for correspondence: A S Markosyan, Faculty of Physics, M V Lomonosov Moscow State University, 119899 Moscow, Russia.

formed with the 3d ions. During the last few years a number of new heterospin metal–radical systems have been reported based on various nitroxide polyradicals, in which each nitroxide group has a spin $S = 1/2$ [5–12].

The heterospin complexes made up of $Mn^{II}(hfac)_2$ (hfac = hexafluoroacetylacetonato ligand) and various π-conjugated nitroxide polyradicals represent a new class of molecule based magnets, which exhibit a large variety of crystal structures and magnetic properties [4, 9]. Thus, the equimolar complexes $[Mn(hfac)_2](\mathbf{2R})$ and $[Mn(hfac)_2](\mathbf{3R_T})\cdot n\text{-}C_6H_{14}$ in which **2R** is *m*-phenylenebis(*N-tert*-butylnitroxide) biradical and $\mathbf{3R_T}$ is a T-shaped triradical bis{3-*tert*-butyl-5-(N-oxy-*tert*-butylamino)phenyl}nitroxide with a triplet and quartet ground state, respectively, have chain structures in which the spins d^5 of Mn(II) and **2R** ($S = 1$) and $\mathbf{3R_T}$ ($S = 3/2$) alternate to form 1D ferrimagnetic chains. By virtue of the weak interchain interaction, the complexes show 3D long range order at 4.5 [13] and 11 K [14], respectively. The 3:2 complex $[Mn(hfac)_2]_3(\mathbf{3R_T})_2$ behaves as a pseudo-3D ferrimagnetic compound with $T_C = 46$ K, in which 1D $\cdots$–Mn(1)–($\mathbf{3R_T}$)–Mn(1)–$\cdots$ chains are coordinatively and exchange linked through the Mn(2) ions via the middle nitroxide group of $\mathbf{3R_T}$ [15, 16].

Since the strength of the exchange interactions is however different in these polyradicals, the complexes show different magnetic properties. Moreover, recent investigations have shown that, depending on interatomic distances and bond angles, the magnitude of the strongest negative Mn–nitroxide interaction can also be varied at least in some of these complexes. Thus, in 1D complexes $[Mn(hfac)_2](\mathbf{2R})$ the exchange integral $J_{R\text{–}Mn}$ was found to be more negative than -350 K, while in the 1D complex $[Mn(hfac)_2](\mathbf{3R_T})\cdot n\text{-}C_6H_{14}$ its value was estimated as -125 K only [17, 18]. The dominating Mn–nitroxide exchange interaction enabled us to isolate linear $(1/2, 5/2, 1/2)$ ferrimagnetic trimers with $S = 3/2$ in these compounds in order to interpret their paramagnetic properties. This approach was also applied to a layered complex $[Mn(hfac)_2]_3(\mathbf{1})_2\cdot n\text{-}C_7H_{16}$ made up of $Mn(hfac)_2$ and a trisnitroxide radical **1** with a threefold symmetry (figure 1), in which the Mn–nitroxide exchange ($J_{R\text{–}Mn} = -175$ K) strongly dominates over the intraradical one [7, 19].

Recently new triradicals with triangular structure, $\mathbf{R}_\Delta$, were obtained and successfully employed for the synthesis of some new complexes with a general formula $[Mn(hfac)_2]_3(\mathbf{R}_\Delta)_2$ [7, 9, 19, 20]. The triradicals all have three ligating sites in a triangular disposition and a quartet ground state (figure 1). The corresponding complexes form stacked 2D-network structures with a hexagonal (**1**) or distorted hexagonal (**2** and **3**) symmetry. The layers are exchange linked with each other to give either ferro/ferrimagnetic or antiferromagnetic 3D long range order at low temperatures (<10 K). In all these compounds the exchange integrals J_1 and J_2 between the nitroxide groups within the ligand molecules are positive, since the radical centres are connected via *m*-phenylene topology. The Mn–nitroxide exchange may be regarded as always negative, $J_{R\text{–}Mn} < 0$.

The magnetic properties of these heterospin complexes are not yet properly understood. Since they have a multi-spin periodicity, even the simplest pair Hamiltonian $H = -2\sum_{i,j} J_{i,j} S_i S_j$ that could describe the magnetic properties of a 1D complex $[Mn(hfac)_2](\mathbf{2R})$ must include six spins, i.e. 576 spin states. The number of states becomes then 13 824 for three $(1/2, 5/2, 1/2)$ units, which needs powerful computational resources. At the same time, isolation of clusters consisting of a small amount of spins is limited by the requirement J(intracluster) $\gg J$(intercluster). Therefore, a comparative analysis of the experimental data collected for compounds of the same kind can facilitate the understanding of their magnetic properties. The series of layered hexagonal complexes $[Mn(hfac)_2]_3(\mathbf{R}_\Delta)_2$ is expected to exhibit a regular change in the magnetic properties. In this paper we present and discuss the magnetic properties of 3:2 complexes of $[Mn(hfac)_2]_3(\mathbf{R}_\Delta)_2$ with trisnitroxide radicals $\mathbf{R}_\Delta = \mathbf{2}$ and **3**. The results are compared with that obtained for $[Mn(hfac)_2]_3(\mathbf{1})_2\cdot n\text{-}C_7H_{16}$ [18].

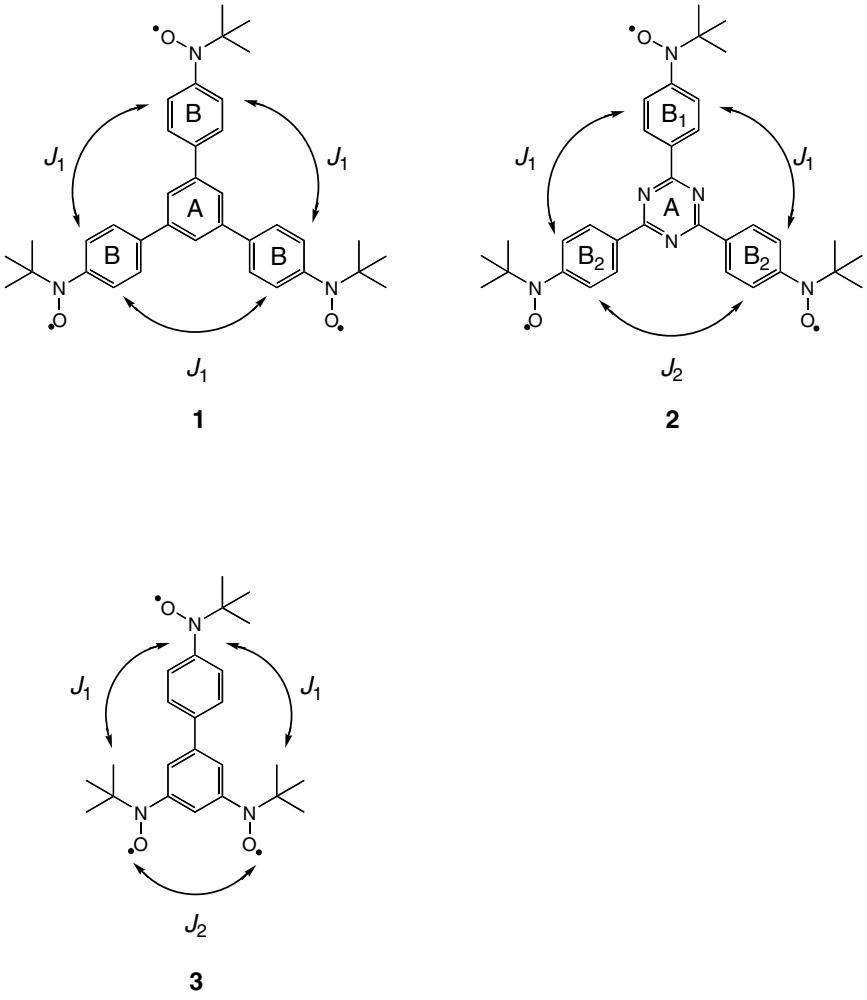

Figure 1. Triangular triradicals **1** ($J_1/k_B = 6.8$ K [22]), **2** ($J_1/k_B = 15.3$ K, $J_2/k_B = 11.8$ K [19]) and **3** ($J_1/k_B \approx 67$ K, $J_2/k_B > 200$ K [20]) with three ligating sites, where A and B indicate the aromatic rings in different positions. J_1/k_B and J_2/k_B were found for the crystals of **1** and **2** or for isolated molecules of **3**. Only the radical **1** has threefold symmetry.

Bivalent Cu^{II} with $S = 1/2$ also forms a honeycomb structure with the trisnitroxides **1** and **2**. The properties of the respective $Cu^{II}(hfac)_2$ complexes are also examined.

The purpose of this work is to disclose the variation of the exchange characteristics and the magnetic dimensionality in these complexes for different triradicals employed. A versatile description of the magnetic properties of this new class of layered molecular magnetic materials is first given.

2. Experiment

The complexes were synthesized by mixing $[Mn(hfac)_2]\cdot 2H_2O$ or $[Cu(hfac)_2]\cdot 2H_2O$ with the radicals **1**, **2** or **3** in an organic solvent benzene, dichlorometane, hexane or *n*-heptane in

inert atmosphere and anhydrous conditions. The solutions were concentrated under reduced pressure and kept subsequently at the temperature −30°C. The reactions were completed by precipitation. The resultant products were deep brown or black powders or crystalline grains of ∼0.1 mm in size. The details of the preparation procedures are described elsewhere [4, 20].

The metal complexes of the triradical **2** always contained solvent molecules. According to the elemental and X-ray structural analyses, benzene molecules were present in the Mn complexes, and the chemical formula was found $[Mn(hfac)_2]_3(\mathbf{2})_2\cdot(C_6H_6)_3$. For the Cu complex crystals of $[Cu(hfac)_2]_3(\mathbf{2})_2\cdot n\text{-}C_6H_{14}$ were obtained.

The magnetization and DC magnetic susceptibility were measured using randomly oriented microcrystals on a SQUID magnetometer MPMS-5S over the temperature range 1.8–350 K and in fields up to 5 T.

3. Summary of the crystal structure

The complexes with radicals **1** and **2** crystallize in a hexagonal structure with the space group $R\bar{3}(h)$. For the same triradical they are isostructural both with Cu and Mn. The crystal structure data of these complexes are given in table 1. In figure 2 the 2D layers of these complexes are shown schematically. In both series, the Mn(II) and Cu(II) ions are octahedrally coordinated by four oxygen atoms of the two (hfac) molecules in *trans* disposition and two oxygen atoms (O1 and O2) of two nitroxide groups belonging to different radicals. The coordination environment is almost same in the complexes of **1** and **2**: the angles Mn–O–N or Cu–O–N remain almost constant, 70 ± 2° (Mn) and 66 ± 2° (Cu). Note that only the triradical **1** has a threefold symmetry in the crystals and the phenylene rings A and B are co-axially rotated in $[Mn(hfac)_2]_3(\mathbf{1})_2\cdot n\text{-}C_7H_{16}$ and $[Cu(hfac)_2]_3(\mathbf{1})_2$. In contrast, the layers of $[Mn(hfac)_2]_3(\mathbf{2})_2\cdot(C_6H_6)_3$ and $[Cu(hfac)_2]_3(\mathbf{2})_2\cdot n\text{-}C_6H_{14}$ consist of two sub-layers, as shown in figure 2(c), and the layer–layer contacts are different in the two series.

Table 1. Crystal structure characteristics of the layered metal–radical complexes.

	Lattice parameters				M–O (of the nitroxide group) distances [Å]		
Compound	*a* [Å]	*c* [Å]	*V* [Å^3]	*Z*	M–O1	M–O2	Character of the layer–layer contacts
$[Mn(hfac)_2]_3(\mathbf{1})_2\cdot n\text{-}C_7H_{16}$[7]	28.462(7)	18.40(1)	12 914(8)	4	2.170	—	By the central phenyl rings (A) of **1** (C–C = 3.60 Å)
$[Mn(hfac)_2]_3(\mathbf{2})_2\cdot(C_6H_6)_3$	23.203(3)	41.839(5)	19 507(3)	6	2.172	2.209	By the O1–O1 (7.02 Å) and O2–O2 (5.73 Å) bonds
$[Cu(hfac)_2]_3(\mathbf{1})_2$	28.425(9)	18.751(8)	13 120(10)	4	2.40	—	By the central phenyl rings (A) of **1** (C–C = 3.66 Å)
$[Cu(hfac)_2]_3(\mathbf{2})_2\cdot n\text{-}C_6H_{14}$	22.980(2)	42.725(3)	19 539(2)	6	2.359	2.451	By the O1–O1 (6.87 Å) and O2–O2 (5.43 Å) bonds

The crystal structure of $[Mn(hfac)_2]_3(\mathbf{3})_2$ is not solved yet. However, based on the chemical structure of the radical **3** and the magnetic data of this complex, it can be suggested as being made up of distorted hexagonal layers as shown in figure 2(d) [20].

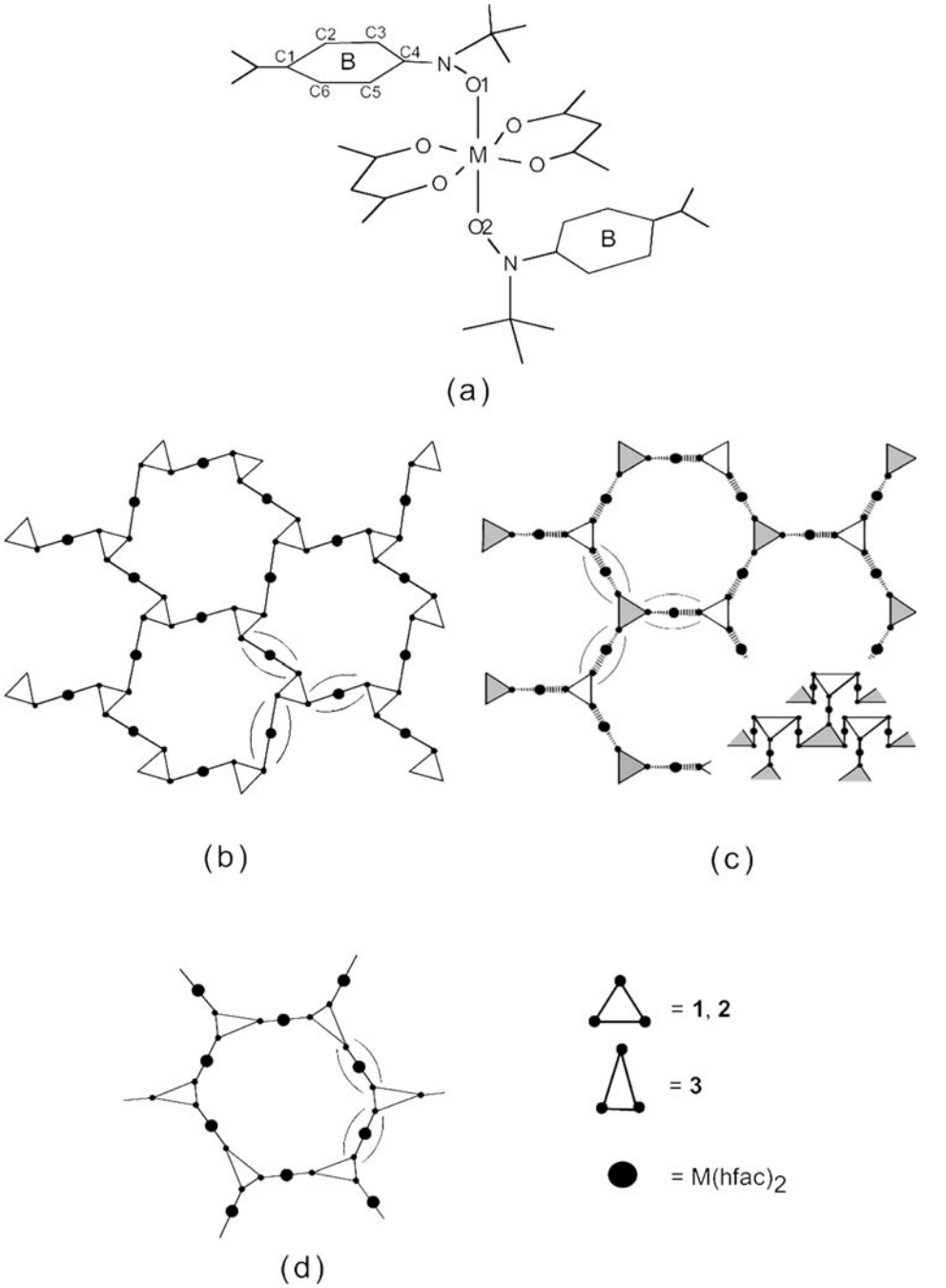

Figure 2. A schematic view of the 2D layers which form complexes with $M(hfac)_2$, M = Mn and Cu. (a) the coordination geometry of the metal and oxygen atoms; (b) $[Mn(hfac)_2]_3(\mathbf{1})_2{\cdot}n\text{-}C_7H_{16}$ and $[Cu(hfac)_2]_3(\mathbf{1})_2$; (c) $[Mn(hfac)_2]_3(\mathbf{2})_2{\cdot}(C_6H_6)_3$ and $[Cu(hfac)_2]_3(\mathbf{2})_2{\cdot}n\text{-}C_6H_{14}$; (d) $[Mn(hfac)_2]_3(\mathbf{3})_2$.

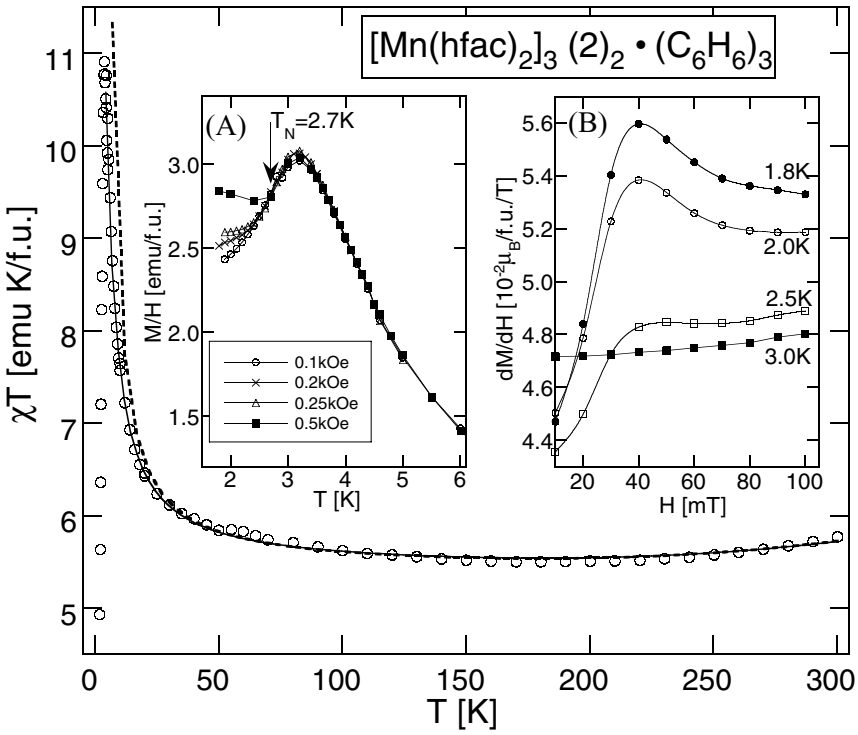

Figure 3. The temperature dependence of the product $\chi_m T$ for the complex $[Mn(hfac)_2]_3(\mathbf{2})_2{\cdot}(C_6H_6)_3$. Open circles are the experimental data. The solid and the dotted lines are the theoretical fits in the 2D and 3D models, respectively (see text). The insets show the low temperature trace of the ratios of magnetization to various magnetic fields (A), and the field derivatives of M against H at different temperatures (B).

4. Magnetic data

The temperature dependence of the product $\chi_m T$ of $[Mn(hfac)_2]_3(\mathbf{2})_2{\cdot}(C_6H_6)_3$ is shown in figure 3. This quantity is proportional to μ_{eff}^2 and can therefore characterize the spin state of the complex. It shows a flat and smeared minimum near 200 K at which $\chi_m T$ reaches 5.33 emu K fu^{-1} (slightly lower than 5.629 emu K fu^{-1} expected for three non-interacting spins $S = 3/2$). With further increasing temperature $\chi_m T$ increases again. This behaviour is similar to what was observed in the complex $[Mn(hfac)_2]_3(\mathbf{1})_2{\cdot}n\text{-}C_7H_{16}$ [18] and can be treated as a temperature induced decay of the (nitroxide–Mn(II)–nitroxide) ferrimagnetic linear trimers with the $(\overline{1/2}, 5/2, \overline{1/2})$ spin configuration, which behave as stable $3/2$ spins at low temperatures. The antiferromagnetic Mn–nitroxide exchange coupling is suggested also in the magnetization curve at low temperature. The magnetization value at 1.8 K reaches 8.2 μ_B/f.u. at 5 T and gradually saturates to 9 μ_B/f.u..

The inset A in figure 3 shows the temperature dependence of the ratio of the magnetization to the magnetic field. They pass through a maximum at 3.2 K and the behaviours change at 2.7 K. The linear field dependence of the magnetization is lost below 2.7 K. Below this temperature, the magnetization curves show a small upturn at low fields, suggesting antiferromagnetic order in this complex with a very weak anisotropy. The Néel point was hence identified as 2.7 K. The critical field of the spin-flop transition was determined by differentiating the magnetic isotherms, as shown in the inset B in figure 3. At 1.8 K the value reaches 400 ± 50 Oe.

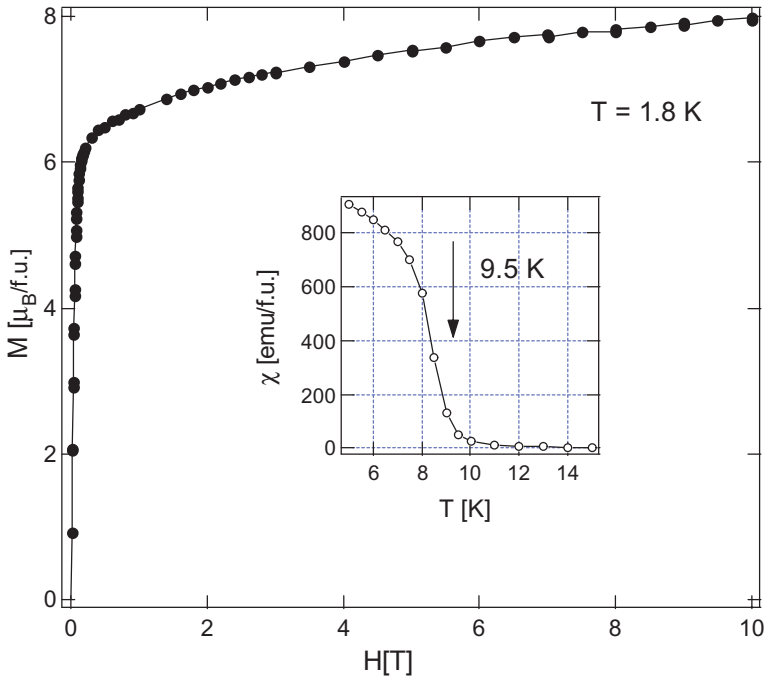

Figure 4. The magnetization curve of the complex [Mn(hfac)$_2$]$_3$(**3**)$_2$ at 1.8 K. The inset shows the low temperature trace of the DC susceptibility measured at 0.5 mT.

The complex [Mn(hfac)$_2$]$_3$(**3**)$_2$ orders ferrimagnetically at $T_C = 9.5$ K [20]. The saturation moment at 1.8 K reaches 9.0 μ_B/f.u. at 2 T, which points to antiferromagnetic coupling between the Mn and radical spins (figure 4). In figure 5, the temperature dependence of the product $\chi_m T$ is shown for this complex. The dependence is characterized by a smooth monotonic decrease with increasing temperature. The high temperature value of $\chi_m T$ approaches asymptotically to the limit 5.625 emu K fu^{-1} expected for three $S = 3/2$ spins per mole. Hence, it can be suggested that the linear ferrimagnetic trimers with the spin configuration $(\overline{1/2}, 5/2, \overline{1/2})$ remain stable up to at least 330 K.

The complexes [Cu(hfac)$_2$]$_3$(**1**)$_2$ and [Cu(hfac)$_2$]$_3$(**2**)$_2$·*n*-C_6H_{14} remain paramagnetic down to 1.8 K. The maximal value of the magnetization found by extrapolation to the infinite external field was close to 9.0 μ_B/f.u. for both, corresponding well to nine coupled $S = 1/2$ spins per fu. Figure 6 displays the temperature dependence of $\chi_m T$ of these complexes. For [Cu(hfac)$_2$]$_3$(**2**)$_2$·*n*-C_6H_{14}, $\chi_m T$ decreases monotonically with increasing temperature; no plateau was seen up to 300 K. In contrast, $\chi_m T$ of [Cu(hfac)$_2$]$_3$(**1**)$_2$ reaches ∼3.5 emu K fu^{-1} above 150 K, which is close to the high temperature limit for nine non-interacting half spins, 3.375 emu K fu^{-1}. This fact indicates essentially weaker exchange couplings in the latter complex. In [Cu(hfac)$_2$]$_3$(**2**)$_2$·*n*-C_6H_{14}, $\chi_m T$ against T shows a maximum at 12 K, which can be accounted for a weak negative interlayer exchange.

5. Analysis and discussion

The relative strength of the exchange interactions in these complexes can be determined by analysing the temperature dependence of $\chi_m T$. For [Mn(hfac)$_2$]$_3$(**2**)$_2$·(C_6H_6)$_3$, the character

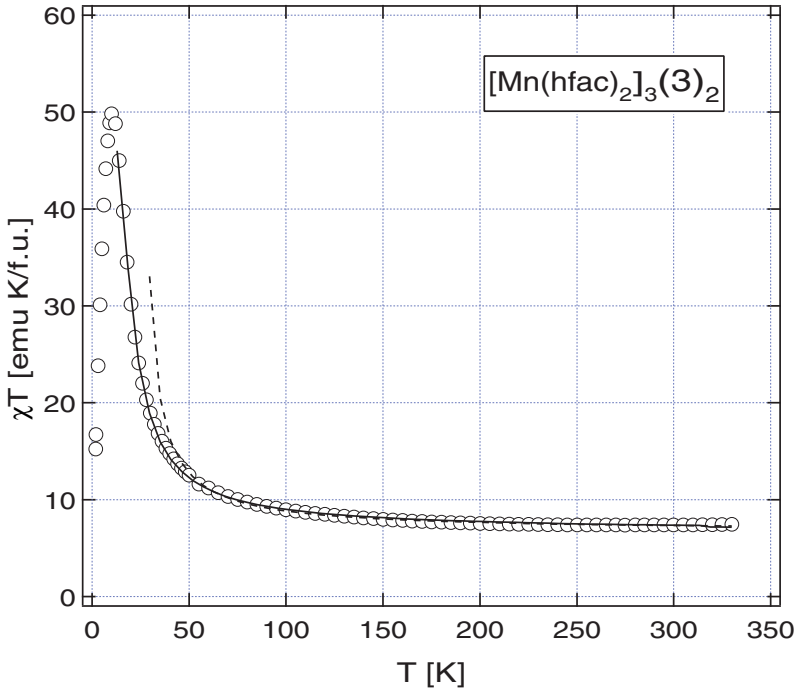

Figure 5. The temperature dependence of $\chi_m T$ for the complex [Mn(hfac)$_2$]$_3$(**3**)$_2$. Open circles are the experimental data. The solid and the dotted lines are the theoretical fits for the 2D and 3D models, respectively.

of the $\chi_m T$–T dependence is similar to that of the complex [Mn(hfac)$_2$]$_3$(**1**)$_2$·*n*-C_7H_{16} [18]. Since over a wide temperature range ∼100–200 K $\chi_m T$ is close to 5.625 emu K fu^{-1}, it can be suggested that the energy levels associated with the excitations of the (nitroxide–Mn(II)–nitroxide) ferrimagnetic spin trimers are not populated at low temperatures and the spin system behaves as if made up of stable 3/2 spins forming 2D honeycomb layers. Above about 200 K the thermal excitations of the trimer spin states become important and $\chi_m T$ starts to increase. These excitations were taken into account by introducing a temperature dependent effective magnetic moment, μ_{eff}, for the trimer spin [16, 18].

In figure 3 the broken curve is a least squares fit to the experimental points using the conventional 3D model in which the intertrimer exchange interaction is treated within the scope of the mean field approximation with the corresponding parameter λ (for three trimers per molecule):

$$\chi_m T = \frac{3}{(Q^{-1} - \lambda/T)}. \tag{1}$$

In this expression,

$$Q = \frac{N_A g^2 \mu_B^2}{3k_B} \times \left(\frac{15}{4} + \frac{5\exp(5J_{R-Mn}/k_B T) + 5\exp(7J_{R-Mn}/k_B T) + 16\exp(12J_{R-Mn}/k_B T)}{2 + 3\exp(5J_{R-Mn}/k_B T) + 3\exp(7J_{R-Mn}/k_B T) + 4\exp(12J_{R-Mn}/k_B T)} \right) \tag{2}$$

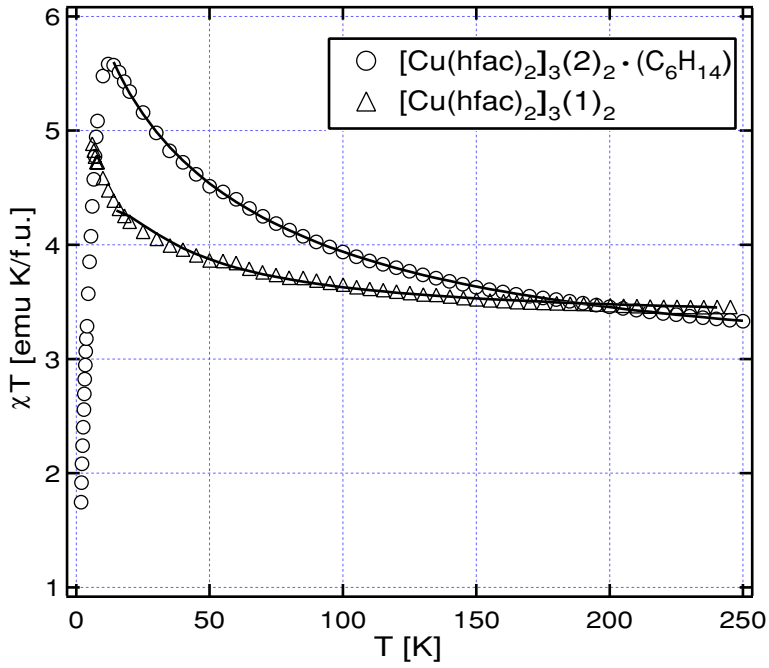

Figure 6. The temperature dependence of $\chi_m T$ for the complexes [Cu(hfac)$_2$]$_3$(**1**)$_2$ (triangular symbols) and [Cu(hfac)$_2$]$_3$(**2**)$_2$·*n*-C$_6$H$_{14}$ (circles). The solid lines are the theoretical fit with the use of the Hamiltonians (4) and (5) (the plots are very close to each other for both the compounds and cannot be distinguished).

is the product χT for an isolated $(\bar{1}/2, 5/2, \bar{1}/2)$ linear trimer, N_A is Avogadro's number and $J_{R\text{–}Mn}$ is the exchange integral of the intratrimer Mn–nitroxide interaction [16]. As seen, the temperature variation of $\chi_m T$ can be explained by the 3D model down to about 30 K only. The best-fitting parameters are $J_{R\text{–}Mn} = -220 \pm 10$ K and $\lambda = 2.5$ emu/f.u. with a purity factor $P = 0.95$ (95%). In this model both the positive intertrimer and negative interlayer interactions are included in λ. Using the power series expansion for a Heisenberg 2D honeycomb lattice with $S = 3/2$ [21] and taking into account the thermal excitations in the nitroxide–Mn(II)–nitroxide trimers, a good fit can be obtained down to T_N (the solid line in figure 3) with the following parameters: $J_{R\text{–}Mn}/k_B = -220 \pm 10$ K, $J'_{3/2-3/2}/k_B = 0.35$ K, $\lambda = -0.711$ emu/f.u. with the purity factor $P = 0.96$. These parameters are quite comparable with those obtained for the complex [Mn(hfac)$_2$]$_3$(**1**)$_2$·*n*-C$_7$H$_{16}$: $J_{R\text{–}Mn}/k_B = -175$ K, $J'_{3/2-3/2}/k_B = 0.23$ K, $\lambda \approx 0$ emu/f.u. [18]. We note that in this approach the intratrimer interaction parameter $J'_{3/2-3/2}$ describes the exchange coupling energy between the integrated spin trimers with $S = \bar{3}/2$, mainly related to the in-plane interactions. This quantity does not correspond the microscopic exchange integral answering the coupling between the radical spins $S = 1/2$, whereas $J_{R\text{–}Mn}$ is the true microscopic exchange integral of the Mn–nitroxide interaction.

The main differences between [Mn(hfac)$_2$]$_3$(**1**)$_2$·*n*-C$_7$H$_{16}$ and [Mn(hfac)$_2$]$_3$(**2**)$_2$·(C$_6$H$_6$)$_3$ are (i) the positive value of λ obtained for the former complex, which reflects the positive interlayer exchange interaction, and (ii) the complex with the triradical **2** shows a clear 2D magnetic behavior below 40 K, while the effect of dimensionality was negligible in the former one [18].

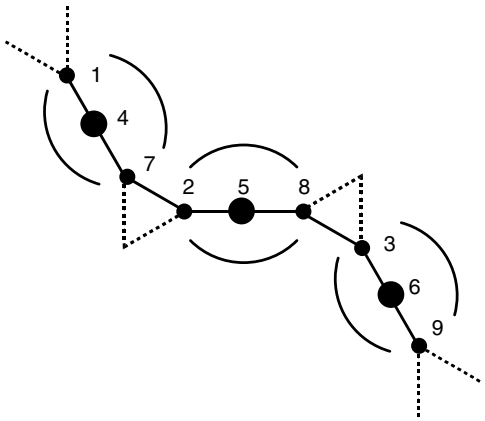

(a)

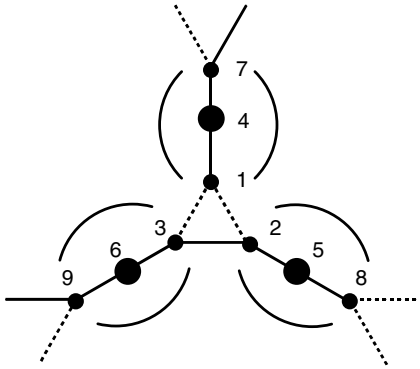

(b)

Figure 7. Two clusters that can be isolated in planes formed by the triangular radicals **1**, **2** and **3** with $Cu(hfac)_2$ and $Mn(hfac)_2$. The solid and dotted lines indicate the stronger and weaker exchange paths, respectively. The numbering of the sites in the clusters (a) and (b) is given according to the Hamiltonians (4) and (5), respectively.

For $[Mn(hfac)_2]_3(\mathbf{3})_2$, $\chi_m T$ can be described satisfactorily by equation (1) above 60 K only (the dashed line in figure 5) with $Q = 15/8$ (stable 3/2 spins), $\lambda = 12.56$ emu/f.u. and $P = 1.2$. A fit over the extended temperature range, 12–330 K, using the power series expansion for a 2D honeycomb Heisenberg lattice made up of stable 3/2 spins gave a better, but still unsatisfactory result. This indicates the importance of lower symmetry of the 2D network for this complex. In the triradical **3**, the exchange coupling J_1 between the two nitroxide groups of the same benzene ring was estimated to exceed 200 K, while J_2, between the nitroxide groups of different benzene rings, is 67 K only [20]. Therefore, the 2D layers of the complex $[Mn(hfac)_2]_3(\mathbf{3})_2$ were thought of as being rhombic planar networks formed by linear nine-spin clusters (figure 7(a)). The power series expansion for a Heisenberg square planar lattice was hence applied [21]. In this model, the nine-spin clusters are formed by three stable 3/2 spins, and the excitations within these (3/2, 3/2, 3/2) trimers were taken into account replacing the product $S(S + 1)$ for $S = 9/2$ by the expression $(3k_B/N_A g^2 \mu_B^2)Q_2$.

$$Q_2 = \frac{N_A g^2 \mu_B^2}{3k_B} \times \left(\frac{3}{4} + 6\frac{11 + 20K^9 + 10K^6 + 4K^3 + 4K^{-1} + K^{-2} + K^{-6} + 4K^{-7} + K^{-12}}{6 + 5K^9 + 4K^6 + 3K^3 + 3K^{-1} + 2K^{-2} + K^{-5} + 2K^{-6} + 3K^{-7} + K^{-9} + 2K^{-12}}\right) \tag{3}$$

is the product χT for an isolated $(3/2, 3/2, 3/2)$ linear trimer, each consisting of nine spins (three spins 5/2 of Mn(II) and six spins 1/2 of radicals **3**), and $K = \exp(J'_{3/2-3/2}/k_B T)$, where $J'_{3/2-3/2}$ corresponds to the intratrimer exchange interaction energy between the integrated spins $S = 3/2$ of the $(3/2, 3/2, 3/2)$ linear trimers. In this model, a good fit was obtained over the range 12–330 K with the following parameters: $J'_{3/2-3/2}/k_B = 7.415$ K, $J''_{9/2-9/2}/k_B = 0.164$ K (this parameter corresponds to the intertrimer in-plane exchange interaction energy), $\lambda = -0.24$ emu/f.u. and $P = 1.15$ (the solid line in figure 5).

The complexes with Cu(II) behave differently. No spin configuration based on stable or quasistable three-spin clusters, either weakly interacting (nitroxide–Cu(II)–nitroxide) linear $(1/2, 1/2, 1/2)$ trimers or triangular trimers formed by the nitroxide spins of the triradicals **1** and **2** weakly interacting with the magnetic sublattice made up of the Cu(II) spins, was found in the paramagnetic range. Both 3D and 2D models were probed. The exchange parameters of these compounds were determined by a numerical simulation of $\chi_m T$ for weakly interacting nine-spin clusters. Considering that the ratio J_1/J_2 of the exchange interactions between the two spins on the side and the base of the isosceles-triangular radical **2** is 0.77, i.e. does not differs much from unity [19], two possible spin configurations were analysed: triangular nine-spin clusters with threefold symmetry shown in figure 7(b), and linear nine-spin clusters similar to those used for the complex [Mn(hfac)$_2$]$_3$(**3**)$_2$ (figure 7(a)). These clusters include both the Cu–nitroxide (J_{R-Cu}) and nitroxide–nitroxide (J_{inR}) exchange interactions as microscopic exchange parameters. The Hamiltonians for configurations (a) and (b) can be written in the Heisenberg form as

$$H = -2J_{inR}\left(\gamma \sum_{i=1}^{6} S_i S_{i+3} + \sum_{i=1}^{2} S_{i+1} S_{i+6}\right) \tag{4}$$

and

$$H = -2J_{inR}\left(\gamma \sum_{i=1}^{6} S_i S_{i+3} + \sum_{i<j=1}^{3} S_i S_i\right) \tag{5}$$

respectively. Here $\gamma = J_{R-Cu}/J_{inR}$.

The susceptibility data for the complexes [Cu(hfac)$_2$]$_3$(**1**)$_2$ and [Cu(hfac)$_2$]$_3$(**2**)$_2$·*n*-C$_6$H$_{14}$ were least-squares fitted with equation (1) where Q was replaced by Q_3:

$$Q_3 = N_A \sum_i (-\partial E_i/\partial H) \exp(-E_i/kT) \left(\sum_i \exp(-E_i/kT)\right)^{-1} \frac{T}{H}. \tag{6}$$

In this equation $\partial E_i/\partial H$ is the change in the energy of the ith level in response to a change in the magnetic field. All the spin values were taken as 1/2 and g-factors equal to 2. The energies of various sub-levels ($\pm M_S$) of the ground state (in total 512 for each cluster) are obtained by direct diagonalization on each iteration of the spin Hamiltonian matrixes of equations (4) and (5), which included also a weak Zeeman term with $H = 0.5$ mT. Both the fits shown in figure 6 by solid lines are indistinguishable down to 15 K and give close values for J_{R-Cu}

and J_{inR} with a weak negative mean field correction. Hence, both the spin configurations can co-exist in this complex simultaneously.

The exchange parameters obtained for the four complexes studied in this work and for $[Mn(hfac)_2]_3(\mathbf{1})_2{\cdot}n\text{-}C_7H_{16}$ are listed in table 2. Considering that for the Mn complexes mean field corrections of different signs were necessary in order to satisfy good fitting conditions, correct estimates of the nitroxide–nitroxide exchange integrals are rather ambiguous. It can nevertheless be noticed that $J'_{3/2-3/2}$ and $J''_{9/2-9/2}$ found for the complex $[Mn(hfac)_2]_3(\mathbf{3})_2$ with the isosceles triradical **3** give a reasonable ratio, $(7.415 \times 9/4)/(0.164 \times 81/4) \approx 5$, when referred to the same numbers of integrated spins, $3/2$ and $9/2$. This ratio is in agreement with the estimate given in [19] for the nitroxide–nitroxide exchange integrals of the free triradical **3**, $J_1/J_2 > 3$. The results also indicate that in the Mn complex with **2** the parameter J_1 is close to J_2 as was found for the free triradical **2** [19].

Table 2. Exchange parameters of the layered metal–radical complexes.

Compound	J_{R-Mn}, J_{R-Cu} (K)	J (intertrimer or intraradical) (K)	λ (emu mol^{-1})	Model	Magnetic ordering and $T_C(T_N)$
$[Mn(hfac)_2]_3$	-175 ± 20		0.333 ± 0.03	3D	FM, 3.4 K
$(\mathbf{1})_2{\cdot}n\text{-}C_7H_{16}$[18]	-175 ± 20	$J'_{3/2-3/2} = 0.226 \pm 0.02$	$\sim 0 \pm 0.5$	2D (honeycomb $3/2$)	
$[Mn(hfac)_2]_3$ $(\mathbf{2})_2{\cdot}(C_6H_6)_3$	-220 ± 20	0.35 ± 0.03	-0.711 ± 0.02	2D (honeycomb $3/2$)	AF, 3.2 K
$[Mn(hfac)_2]_3(\mathbf{3})_2$	<-350	$J'_{3/2-3/2} = 7.415 \pm 0.2$ $J''_{9/2-9/2} = 0.164 \pm 0.02$	-0.24 ± 0.02	2D (squire $9/2$)	FM, 9.5 K
$[Cu(hfac)_2]_3(\mathbf{1})_2$	$+16 \pm 2$	$J_{inR} = 1.6 \pm 0.2$	-0.55 ± 0.2	nine-spin cluster	<1.8 K
$[Cu(hfac)_2]_3$ $(\mathbf{2})_2{\cdot}n\text{-}C_6H_{14}$	$+77 \pm 3$	$J_{inR} = 14.5 \pm 1$	-0.2 ± 0.02	nine-spin cluster	<1.8 K

For $[Cu(hfac)_2]_3(\mathbf{2})_2{\cdot}n\text{-}C_6H_{14}$ the exchange parameters obtained with the use of the Hamiltonians (4) and (5) do not depend on the temperature range of the fit down to 15 K. Hence, the nine-spin cluster model was suggested as a good approximation for this complex above 15 K (at lower temperatures larger clusters must be considered). The exchange parameters for this complex listed in table 2 can therefore be considered as being close to the values expected for infinite 2D layers. In this complex, the value of J_{inR} is the average of the three interactions $J_{inR} \approx (2J_1 + J_2)/3 = 14.1$ K. I.e., the exchange interaction between the nitroxide groups of the free triradical **2** remains almost unchanged in the respective 2D complex. In contrast, J_{inR} in $[Cu(hfac)_2]_3(\mathbf{1})_2$ is substantially lower than 6.8 K, the value found for a free radical **1** [22]. This can be attributed to a substantial distortion of the radical bond angles in the complex. In a free radical **1** the rotation angle between the A and B benzene rings is 19.5°, while in the complex it is 29.7°. Also the dihedral angle between the (C4–C5–N1) and (C4–N1–O1) planes (see figure 2(a)) is 37.4° in the free triradical **1** and changes to 14.7° in the complex. The quality of the fits for $[Cu(hfac)_2]_3(\mathbf{2})_2{\cdot}n\text{-}C_6H_{14}$ was better than for $[Cu(hfac)_2]_3(\mathbf{1})_2$. Therefore, another reason for the lower value of J_{inR} determined for the $[Cu(hfac)_2]_3(\mathbf{1})_2$ complex can be underestimation of this parameter when using the above cluster models (as table 2 shows, the mean field correction for this complex is higher that for the Cu complex with **2**). These arguments can also be applied to the Mn complex with **1**, $[Mn(hfac)_2]_3(\mathbf{1})_2{\cdot}n\text{-}C_7H_{16}$, which

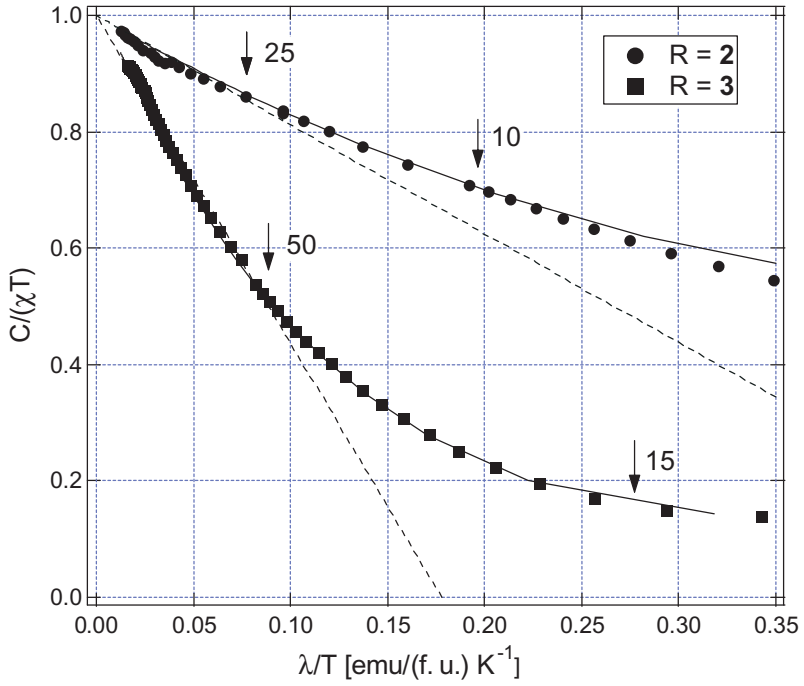

Figure 8. $C/(\chi T)$-λ/T plots for $[Mn(hfac)_2]_3(\mathbf{2})_2{\cdot}(C_6H_6)_3$ and $[Mn(hfac)_2]_3(\mathbf{3})_2$. The solid and dotted lines show the behaviour for the 2D and 3D models, respectively. Some temperatures are indicated by arrows for clarity.

does not show low dimensionality either [18]. In this complex the intraradical exchange interaction can also be weakened substantially.

The Cu(II)–nitroxide interaction is also variable in the complexes, 16 and 77 K, for $\mathbf{3R}_\Delta = \mathbf{1}$ and **2**, respectively. The value of J_{R-Cu} found in the seven-unit cluster complex $[Cu(hfac)_2]_3(\mathbf{4})_2$ with similar building blocks as shown in figure 2(a), where **4** is the 5-bromo-1,3-bis(*N-tert*-butylnitroxide)benzene diradical, was found to be about 30 K [23].

In contrast to $[Mn(hfac)_2]_3(\mathbf{1})_2{\cdot}n\text{-}C_7H_{16}$, the Mn complexes with radicals **2** and **3** show a clear 2D behavior. Figure 8 shows the temperature variation of the magnetic susceptibility for the complexes $[Mn(hfac)_2]_3(\mathbf{2})_2{\cdot}(C_6H_6)_3$ and $[Mn(hfac)_2]_3(\mathbf{3})_2$ in the $C/(\chi T)$–λ/T presentation (C being the Curie constant), which displays better the low temperature behaviour. As seen, the effect of low dimensionality is more pronounced in the latter compound, with stronger nitroxide–nitroxide exchange. For the heterospin systems under discussion the two-dimensionality depends on the weakest in-plane exchange, which in turn must dominate over the interplane exchange interaction. Hence, the dimensionality of these systems is driven mainly by the intraradical exchange. The intraradical nitroxide–nitroxide exchange interaction is very weak in $[Mn(hfac)_2]_3(\mathbf{1})_2{\cdot}n\text{-}C_7H_{16}$, which hardly shows two-dimensionality. Therefore, the cause of the 2D behaviour in these layered complexes can be associated with the increasing intraradical exchange interactions along the sequence of the radicals **1**, **2** and **3**.

The results presented show that these layered compounds have qualitatively different magnetic behaviour both in the paramagnetic temperature range as well as in the ordered state. While all the Mn-based complexes have similar spin arrangement within the layers, the interlayer interactions have different signs in them. This can be ascribed to the different

character of the interlayer coupling (see table 1). While the nitroxide–nitroxide contacts are the closest and can provide a negative interlayer exchange coupling in $[Mn(hfac)_2]_3(\mathbf{2})_2\cdot(C_6H_6)_3$ and $[Cu(hfac)_2]_3(\mathbf{2})_2\cdot n\text{-}C_6H_{14}$, the magnetic orbitals are essentially separated in space (the nearest contacts are through the phenyl A rings) in $[Mn(hfac)_2]_3(\mathbf{1})_2\cdot n\text{-}C_7H_{16}$, making a positive interlayer coupling possible. The same reason may be a cause of the positive interlayer interaction in the complex $[Mn(hfac)_2]_3(\mathbf{3})_2$.

6. Conclusion

New layered heterospin metal radical complexes with three-spin periodicity made up of $Mn(hfac)_2$ and $Cu(hfac)_2$ and different triangular nitroxide radicals show various magnetic properties depending on details of the crystal structure and exchange paths. They are characterized by weak anisotropy. With the triradicals **2** and **3** having a comparatively strong nitroxide–nitroxide exchange, the complexes show a clear 2D behaviour in the paramagnetic temperature range. Due to the dominating Mn–nitroxide exchange, the exchange integral J_{R-Mn} can be determined by isolation of quasistable linear trimers and using analytical expressions.

Acknowledgments

This work was supported in part by a Grant-in-Aid for Scientific Research on Priority Areas of Molecular Conductors and Magnets (Area No 730/11224214) from the Ministry of Education, Science, Sport and Culture, Japan. ASM is indebted to the Ministry of Education, Science and Culture, Japan, for the financial support.

References

[1] Ch J O'Connor (ed) 1993 *Research Frontiers in Magnetochemistry* (Singapore: World Scientific)
[2] E Coronado, P Delhaès, D Gatteschi and J S Miller (ed) 1996 *Molecular Magnetism: from Molecular Assemblies to the Devices (NATO ASI Series E Vol. 321)* (Dordrecht: Kluwer)
[3] M Kitano, Y Ishimaru, K Inoue, N Koga and H Iwamura 1994 *Inorg. Chem.* **33** 6012
[4] H Iwamura and K Inoue 2000 *Magnetoscience—From Molecules to Materials* ed J S Miller and M Drillon (Weinheim: Wiley–VCH)
[5] Eaton G R and Eaton S S 1988 *Accounts Chem. Res.* **21** 107
[6] Nakamura N, Inoue K, Iwamura H, Fujioka T and Sawaki Y 1992 *J. Am. Chem. Soc.* **114** 1484
[7] Inoue K and Iwamura H 1994 *J. Am. Chem. Soc.* **116** 3173
[8] Ovcharenko V, Burdukov A and Musin R 1995 *Mol. Cryst. Liq. Cryst.* **273** 88
[9] Iwamura H, Inoue K and Koga N 1998 *New J. Chem.* **22** 201
[10] Blundell S J, Pattenden P A, Pratt F L, Chow K H, Hayes W and Sugano T 1997 *Hyperfine Interact.* **104** 251
[11] Fegy K, Luneau D, Rey P, Ohm T and Paulsen C 1998 *Angew. Chem. Int. Edn. Engl.* **37** 1270
[12] Decurtins S, Schmalle H and Pellaux R 1998 *New. J. Chem.* **22** 117
[13] Inoue K and Iwamura H 1994 *J. Chem. Soc. Chem. Commun.* 2273
[14] Inoue K, Hayamizu T and Iwamura H 1995 *Chem. Lett.* 745
[15] Inoue K, Hayamizu T, Iwamura H, Hashizume D and Ohashi Y 1996 *J. Am. Chem. Soc.* **118** 1803
[16] Markosyan A S, Hayamizu T, Iwamura H and Inoue K 1998 *J. Phys.: Condens. Matter* **10** 2323
[17] Inoue K, Iwahori F, Markosyan A S and Iwamura H 2000 *Coord. Chem. Rev.* **198** 219
[18] Markosyan A S, Hosokoshi Y and Inoue K 1999 *Phys. Lett.* A **261** 212
[19] Hayami S and Inoue K 1999 *Chem. Lett.* 545
[20] Inoue K and Iwamura H 1996 *Adv. Mater.* **8** 73
[21] Navarro R 1990 *Magnetic Properties of Layered Compounds* ed L J de Jongh (Dordrecht: Kluwer) p 105
[22] Kanno F, Inoue K, Koga N and Iwamura H 1993 *J. Phys. Chem.* **97** 13267
[23] Inoue K, Iwahori F and Iwamura H 1998 *Chem. Lett.* 737